Preparation of 6-((*N*-3,5-Dimethylpyrazolyl)methyl)-2,2'-bipyridine (6b). Reaction of a mixture of **10** and **11** (450 mg) with 3,5-dimethylpyrazole (224 mg) according to the above procedure gave 6-(*N*-3,5-dimethylpyrazolyl)methyl-2,2'-bipyridine (**6b**) as a colorless solid, mp 85-88 °C. Anal. Calcd for $C_{16}H_{16}N_4 \cdot {}^1/_2H_2O$: C, 70.31; H, 6.27; N, 20.49. Found: C, 69.69; H, 5.86; N, 20.00. ^{1}H NMR ($CDCl_3$): 8.68, d, H6'; 8.39, d, H3'; 8.27, d, H3; 7.82, t, H4'; 7.74, t, H4; 7.31, m, H5'; 6.82, d, H5; 5.90, s, H4''; 5.42, s, $-CH_2$; 2.27, s, 3''-CH_3; 2.25, s, 5''-CH_3. ^{13}C NMR ($CDCl_3$): 149.2, C6'; 138.0, C4; 136.9, C4'; 123.7, C5'; 121.2, C3'; 120.9, C5; 119.7, C3; 105.7, C4''; 54.5, $-CH_2$; 13.5 and 11.2, C3''- and C5''-CH_3.

Preparation of Ruthenium Complexes. General Procedure. To a solution of $RuCl_3 \cdot 3H_2O$ (1.0 mmol) in ethanol-water (90:10; 25 mL) was added the ligand (2.0 mmol), and the mixture was heated at reflux under a nitrogen atmosphere for 72 h. The solvent was then removed by rotary evaporation and the residue dissolved in water. The crude product was precipitated by dropwise addition of an ammonium hexafluorophosphate solution. Purification was by recrystallization from acetonitrile/diethyl ether or by column chromatography. ^{1}H and ^{13}C NMR spectra are given in Table I. Electronic spectra and redox potentials are listed in Table II.

(i) Reaction of **5a** as above gave bis[6-(*N*-pyrazolyl)-2,2'-bipyridine-*N*,*N'*,N2'']ruthenium(II) hexafluorophosphate (**12a**) as an orange-red solid in 55% yield. Anal. Calcd for $C_{26}H_{20}N_8RuP_2F_{12}$: C, 37.38; H, 2.41; N, 13.41. Found: C, 37.11; H, 2.17; N, 13.31.

(ii) Reaction of **5b** as above gave bis[6-(*N*-2,5-dimethylpyrazolyl)-2,2'-bipyridine-*N*,*N'*,*N2''*]ruthenium(II) hexafluorophosphate (**12b**) as a dark red solid in 50% yield. Anal. Calcd for $C_{30}H_{28}N_8RuP_2F_{12} \cdot CH_3CN$: C, 41.13; H, 3.34; N, 13.49. Found: C, 41.27; H, 3.06; N, 13.70.

(iii) Reaction of **6a** as above gave bis[6-(*N*-pyrazolyl)methyl-2,2'-bipyridine-*N*,*N'*,*N2''*]-ruthenium(II) hexafluorophosphate (**13a**) as a red solid in 67% yield. Anal. Calcd for $C_{28}H_{24}N_8RuP_2F_{12}$: C, 38.95; H, 2.80; N, 12.98. Found: C, 38.63; H, 2.95; N, 12.80.

(iv) Reaction of **6b** as above gave a red solid, which ^{1}H NMR showed to be a mixture of **13b** and **14**. Chromatography on alumina using chloroform/methanol as eluting solvents gave first bis[6-(*N*-3,5-dimethylpyrazolyl)methyl-2,2'-bipyridine-*N*,*N'*,*N2''*]ruthenium(II) hexafluorophosphate (**13b**), followed by chloro[6-(*N*-3,5-dimethylpyrazolyl)methyl-2,2'-bipyridine-*N*,*N'*,*N2''*][6-(*N*-3,5-dimethylpyrazolyl)methyl-2,2'-bipyridine-*N*,*N'*]ruthenium(II) hexafluorophosphate (**14**). ^{1}H NMR (CD_3CN) for the tridentate ligand: 8.51, d, H3; 8.33, d, H3'; 8.19, t, H4; 8.01, d, H5; 7.81, t, H4'; 7.30, d, H6'; 7.26, t, H5'; 5.79, s, H4''; 5.55, d, and 6.23, d, CH_2; 2.57, s, 5''-CH_3; 1.14, s, 3''-CH_3. ^{1}H NMR (CD_3CN) for the bidentate ligand: 10.30, d, H6'; 8.55, d, H3'; 8.29, t, H4'; 8.19, d, H3; 7.89, t, H5'; 7.62, t, H4; 6.03, d, H5; 6.00, s, H4''; 3.58, d, and 3.93, d, CH_2; 2.07, s, 3''-CH_3; 1.43, s, 5''-CH_3. ^{13}C NMR (CD_3CN): 155.5, 152.3, 138.1, 137.9, 137.8, 136.6, 127.4, 127.2, 125.4, 124.4, 124.1, 123.5, 122.5, 106.9, 104.0, 52.5, 52.3, 14.0, 13.4, 12.3, 10.3.

Contribution from the Department of Chemistry, University of Houston, Houston, Texas 77204-5641

Evaluation of Electron-Transfer Sites in Ruthenium(II) Octaethylporphyrin Complexes of the Type (OEP)Ru(CO)(L)

K. M. Kadish,* P. Tagliatesta, Y. Hu, Y. J. Deng, X. H. Mu, and L. Y. Bao

Received February 13, 1991

(OEP)Ru(CO) and (OEP)Ru(CO)(L) (where OEP = the dianion of octaethylporphyrin and L = an axial ligand) were electrochemically characterized in seven different nonaqueous solvents. The investigated complexes undergo two oxidations and either one or two reductions depending upon solvent. Both oxidations are ring centered, but this is not the case for reductions, which occur at either the porphyrin π-ring system or the central metal ion depending upon the specific solution conditions and the sixth axial ligand. An overall Ru(II) → Ru(I) reaction is suggested by thin-layer UV-visible spectroelectrochemical data in PhCN, CH_3CN or PrCN, while π-ring-centered reductions are suggested for the first reduction of (OEP)Ru(CO) in DMSO or py. Both reactions can be observed in THF with the initial reduction being ring centered followed by a conversion of the Ru(II) π anion radical to a Ru(I) form of the complex.

Introduction

The spectroscopic properties[1-4] and redox potentials[5-8] for oxidation and reduction of (OEP)Ru(CO)(L) (where OEP is the dianion of octaethylporphyrin and L is an axial ligand) have been extensively investigated over the last two decades. As a result of these studies, the formation of porphyrin π cation radicals and dications has been fairly well documented under a variety of experimental conditions. However, almost no data are available for singly reduced complexes of (OEP)Ru(CO)(L).

The one-electron reduction of (TPP)Ru(CO)(L) and ((*p*-X)-TPP)Ru(CO)(L) (where TPP = the dianion of tetraphenylporphyrin and L is a nitrogeneous base or solvent molecule) occurs at the porphyrin π-ring system and generates a Ru(II) porphyrin π anion radical,[9-12] which has been spectroscopically identified.[11] It was expected that (OEP)Ru(CO)(L) would also be reduced at the porphyrin macrocycle, but recent UV-visible data suggested that the electroreduction of (OEP)Ru(CO) in THF occurs at the metal center to give a Ru(I) porphyrin complex on the spectroelectrochemical time scale.[13] This reaction is investigated in the present paper, which characterizes (OEP)Ru(CO) redox reactions in seven different nonaqueous solvents. Each electroreduction and selected electrooxidations were investigated by thin-layer UV-visible and FTIR spectroelectrochemistry.

Experimental Section

Instrumentation and Procedure. Solution infrared spectra were measured by using an IBM 32 FTIR spectrometer and a light-transparent FTIR spectroelectrochemical cell whose construction has been described in the literature.[14] Thin-layer UV-visible spectroelectrochemical ex-

(1) Antipas, A.; Buchler, J. W.; Gouterman, M.; Smith, P. D. *J. Am. Chem. Soc.* **1978**, *100*, 3015.
(2) Barley, M.; Dolphin, D.; James, B. R.; Kirmaier, C.; Holten, D. *J. Am. Chem. Soc.* **1984**, *106*, 3937.
(3) Eaton, G. R.; Eaton, S. S. *J. Am. Chem. Soc.* **1975**, *97*, 235.
(4) Crawford, B. A.; Ondrias, M. R. *J. Phys. Chem.* **1989**, *93*, 5055.
(5) (a) Brown, G. M.; Hopf, F. R.; Ferguson, J. A.; Meyer, T. J.; Whitten, D. G. *J. Am. Chem. Soc.* **1973**, *95*, 5939. (b) Brown, G. M.; Hopf, F. R.; Meyer, T. J.; Whitten, D. G. *Ibid.* **1975**, *97*, 5385.
(6) Smith, P. D.; Dolphin, D.; James, B. R. *J. Organomet. Chem.* **1981**, *208*, 239.
(7) Barley, M.; Becker, J. Y.; Domazetis, G.; Dolphin, D.; James, B. R. *J. Chem. Soc., Chem. Commun.* **1981**, 982.
(8) Barley, M.; Becker, J. Y.; Domazetis, G.; Dolphin, D.; James, B. R. *Can. J. Chem.* **1983**, *61*, 2389.
(9) Kadish, K. M.; Chang, D. *Inorg. Chem.* **1982**, *21*, 3614.
(10) Malinski, T.; Chang, D.; Bottomley, L. A.; Kadish, K. M. *Inorg. Chem.* **1982**, *21*, 4248.
(11) Mu, X. H.; Kadish, K. M. *Langmuir* **1990**, *6*, 51.
(12) Rillema, D. P.; Nagle, J. K.; Barringer, L. F., Jr.; Meyer, T. J. *J. Am. Chem. Soc.* **1981**, *103*, 56.
(13) Kadish, K. M.; Mu, X. H. *Pure Appl. Chem.* **1990**, *62*, 1051.
(14) Kadish, K. M.; Mu, X. H.; Lin, X. Q. *Electroanalysis* **1989**, *1*, 35.

0020-1669/91/1330-3737$02.50/0

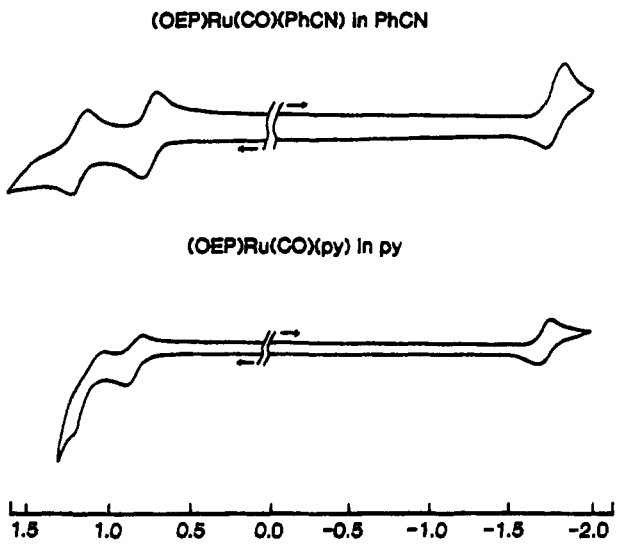

Figure 1. Cyclic voltammograms of (OEP)Ru(CO) in PhCN and py containing 0.1 M TBAP. Scan rate = 10 V/s.

periments were carried out with a vacuum-tight thin-layer spectroelectrochemical cell.[15] A Tracor Northern 1710 holographic optical spectrometer/multichannel analyzer or Tracor Northern 6500 rapid-scan spectrometer was used to obtain thin-layer UV–visible spectra in the time-resolved mode. Controlled-potential electrolysis was performed with a PAR Model 174A polarographic analyzer or an IBM 225A voltammetric analyzer coupled with Princeton Applied Research Model RE 0074 X-Y recorder. Microvoltammetric experiments were carried out inside a well-grounded Faraday cage with a homemade potentiostat that was driven by a PAR Model 175 universal programmer. A Tektronix Model 5111 storage oscilloscope and a Tektronix Model CS-A camera were used to record current–voltage curves. Cyclic voltammograms were obtained at several different Pt button electrodes whose diameters ranged from ~1 mm to 25 μm. The auxiliary electrode was also made of platinum and a saturated calomel electrode (SCE) was used as the reference electrode.

Solutions for the spectroelectrochemical measurements contained 0.2 M tetra-*n*-butylammonium perchlorate (TBAP) as supporting electrolyte, while those for cyclic voltammetry contained 0.1 M TBAP. Deaeration was performed by passing a stream of nitrogen or argon gas saturated with the solvent being used through the solution for 5–10 min and then maintaining a positive pressure of the inert gas over the solution while the measurements were made.

Chemicals. Each nonaqueous solvent was freshly distilled under nitrogen or argon or, alternatively, vacuum-distilled before use. Spectroscopic grade methylene chloride (CH_2Cl_2) was distilled over P_2O_5. Pyridine (py) was freshly distilled over CaH_2 under an argon atmosphere. Benzonitrile (PhCN) and dimethyl sulfoxide (DMSO) were freshly distilled over activated 4-Å molecular sieves. Acetonitrile (CH_3CN) (H_2O < 0.005%) and analytical grade *n*-butyronitrile (PrCN) were purchased from Aldrich Chemical Co. and used as received. Commercial grade tetrahydrofuran (THF) was passed through an activated alumina column and then dried and distilled from CaH_2 or $LiAlH_4$ under N_2. Only the $LiAlH_4$ treatment gave a rigorously dried solution. (OEP)Ru(CO) was prepared by using a procedure similar to the one described for the synthesis of (TPP)Ru(CO)[11] and was recrystallized from a chloroform/methanol mixture as a six-coordinate CH_3OH adduct.[16] A commercial sample of (OEP)Ru(CO)(THF)[16] was purchased from Aldrich Chemical Co. and was either used without further purification or recrystallized from a 1:1 THF/*n*-hexane mixture.

Results

Electrode Reactions of (OEP)Ru(CO). Cyclic voltammograms of (OEP)Ru(CO)(L) in PhCN and py containing 0.1 M TBAP are shown in Figure 1. Two oxidations are observed in both solvents. One reduction is observed in PhCN while two are

Table I. Half-Wave Potentials (V vs SCE) for Reduction and Oxidation of (OEP)Ru(CO) in Selected Solvents Containing 0.1 M TBAP with Scan Rate = 10 V/s

	oxidn			redn		
solvent	1st	2nd	$\Delta E_{1/2}$, V	1st	2nd	$\Delta E_{1/2}$, V
CH_2Cl_2[a]	0.68	1.12	0.44	−1.72[c]	−2.09[c]	0.37
PhCN[a]	0.77	1.22	0.45	−1.77		
CH_3CN[b]	0.66	1.04	0.38	−1.73[d]		
PrCN[b]	0.70	1.14	0.44	−1.77	−2.16[e]	
THF[a]	0.87	1.28	0.39	−1.72	−2.20	0.48
DMSO[b]	0.77			−1.64		
py[a]	0.80	1.12	0.32	−1.76	−2.13	0.37

[a] Measured at a 25-μm Pt electrode. Scan rate = 10 V/s. [b] Measured at a conventional electrode. Scan rate = 0.1 V/s. [c] Scan rate = 50 V/s. The first reduction is irreversible due to a reaction involving electrogenerated $[(OEP)Ru(CO)]^-$ and CH_2Cl_2. [d] Reaction is reversible only at scan rates ≥ 0.3 V/s. [e] E_{pc}.

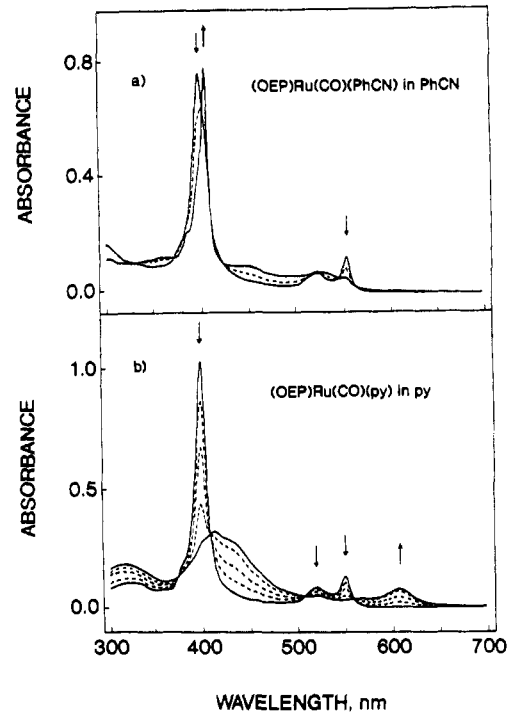

Figure 2. Time-resolved thin-layer UV–visible spectra obtained during controlled-potential reduction of (OEP)Ru(CO) at −1.90 V (a) in PhCN and (b) in py containing 0.2 M TBAP.

monitored in pyridine by cyclic voltammetry at a Pt electrode. (Only the first reduction is illustrated in Figure 1.) Two reductions are also observed at a microelectrode in CH_2Cl_2, PrCN, or THF, and the half-wave or peak potentials for each of these reactions are listed in Table I.

The absolute potential separation between the two reductions of (OEP)Ru(CO)(L) ranges from 0.37 V in CH_2Cl_2 to 0.48 V in THF and is close to the 0.42 ± 0.05 V separation generally observed for porphyrin π-ring-centered reductions of octaethylporphyrin complexes.[17] The difference in $E_{1/2}$ between the first oxidation and the first reduction of (OEP)Ru(CO)(L) ranges from 2.59 V in THF to 2.39 V in CH_3CN, and these values may be compared to a 2.25 ± 0.15 V separation that is generally observed for porphyrin π-ring-centered electron-transfer reactions of OEP complexes.[17]

UV–Visible Monitoring of (OEP)Ru(CO) Reduction. The electroreduction of (OEP)Ru(CO)(L) was investigated by thin-layer spectroelectrochemistry in six different nonaqueous solvents. No measurements were made in CH_2Cl_2, since the overall reduction is irreversible under these solution conditions and leads

(15) Lin, X. Q.; Kadish, K. M. *Anal. Chem.* **1985**, *57*, 1498.
(16) The sixth axial ligand, THF or CH_3OH, was verified by thermogravimetric analysis (TGA), which gave values consistent with the binding of one solvent molecule.
(17) Fuhrhop, J.-H.; Kadish, K. M.; Davis, D. G. *J. Am. Chem. Soc.* **1973**, *95*, 5140.

Table II. UV–Visible and IR Spectral Characteristics of (OEP)Ru(CO) and Electrogenerated [(OEP)Ru(CO)]$^-$ in Solutions Containing 0.2 M TBAP

compd	solvent	λ_{max}, nm ($10^{-4}\epsilon$)						ν_{CO}, cm^{-1} [a]
(OEP)Ru(CO)	CH_2Cl_2	394 (22.0)	516 (1.8)	547 (4.4)				1923
	PhCN	396 (20.8)	519 (2.1)	549 (2.8)				1931
	CH_3CN	392 (26.8)	516 (2.2)	547 (3.6)				1927
	PrCN	395 (23.5)	517 (1.6)	548 (3.1)				1931
	THF[b]	392 (24.1)	516 (3.4)	547 (4.9)				1931
	DMSO	395 (23.8)	517 (1.8)	549 (3.2)				1906
	py	396 (23.1)	519 (2.2)	549 (3.1)				1931
[(OEP)Ru(CO)]$^-$	PhCN	405 (24.7)	521 (2.8)	553 (1.9)				*d*
	CH_3CN[c]	402 (32.1)	524 (2.9)	550 (2.1)				*d*
	PrCN	403 (20.5)	527 (1.4)	548 (2.3)				*d*
	THF[e]	406 (19.3)	520 (2.8)	550 (2.0)	601 (1.0)			1896
	THF[f]	410 (4.3)	432 (4.3)		601 (2.9)	786 (wb)[g]	880 (2.3)	1878
	DMSO	413 (6.9)	437 (7.5)		603 (2.2)	797 (wb)[g]	867 (2.3)	*d*
	py	413 (7.3)	432 (7.2)		606 (1.8)	793 (wb)[g]	885 (1.6)	1896

[a] Values given to ±1 cm^{-1}. [b] No spectral differences in the initial Ru(II) complex were observed as a function of the sixth axial ligand, L. [c] The spectrum is not reversibly converted to that of the original (OEP)Ru(CO)(CH_3CN) species after reoxidation. [d] Values could not be obtained due to solvent and/or compound decomposition during prolonged electrolysis (see text). [e] Recrystallized from CH_3OH. [f] Recrystallized from THF (commercial sample). [g] wb = weak and broad peak.

to several uncharacterized solvent addition products at all potential scan rates less than 20 V/s.

The thin-layer spectral changes that occur upon controlled-potential reduction of (OEP)Ru(CO)(L) in PhCN and pyridine are depicted in Figure 2, while Table II summarizes the spectral properties for neutral and singly reduced (OEP)Ru(CO)(L) in each investigated solvent. The shape of the spectra for the neutral complexes of (OEP)Ru(CO)(L) are similar in all six solvents, but this is not the case after addition of one electron, where two different types of UV–visible spectra are obtained. The spectral changes in PhCN (Figure 2a) are similar to those observed in PrCN or CH_3CN while the changes in pyridine (Figure 2b) are similar to those observed in DMSO. Both sets of spectra pass through several isosbestic points, indicating the presence of only two spectroscopically detectable species in solution. In addition, the UV–visible changes are reversible in each solvent except for CH_3CN (which shows an irreversible cyclic voltammogram) and the initial (OEP)Ru(CO)(L) spectrum could be regenerated by application of a positive controlled potential.

The spectral changes observed in PhCN (Figure 2a), PrCN, or CH_3CN are similar to changes that occur upon conversion of Ag(II) to Ag(I) in (TPP)Ag,[18] and this suggests the formation of a ruthenium(I) porphyrin on the spectroelectrochemical time scale. On the other hand, the final spectrum in pyridine (Figure 2b) or DMSO is characterized by a decreased intensity Soret band and the appearance of two broad bands centered at 603–606 and 867–885 nm. Both spectra resemble those of a porphyrin π anion radical.

The UV–visible spectra obtained after electroreduction of (OEP)Ru(CO)(L) in THF vary as a function of the sixth axial ligand, L, and show properties of a porphyrin π anion radical, a ruthenium(I) porphyrin complex, or both. They also depend upon the solution conditions and the time elapsed after application of an applied potential. Reduction of the THF complex, (OEP)-Ru(CO)(THF), in rigorously dry THF gives a π-anion-radical type spectrum (Figure 3a), while reduction of the CH_3OH adduct, (OEP)Ru(CO)(CH_3OH), leads to the type of UV–visible spectral changes expected for a metal-centered reduction. The final spectrum after reduction of (OEP)Ru(CO)(CH_3OH) in THF has bands at 406, 520, and 550 nm (see Figure 3b) and is similar to the one obtained after reduction of (OEP)Ru(CO) in PrCN, PhCN, or CH_3CN (see Table II). The UV–visible spectrum of singly reduced (OEP)Ru(CO)(THF) could be converted to the spectrum of singly reduced (OEP)Ru(CO)(CH_3OH) by adding several drops of CH_3OH or H_2O to solution,[19] and the resulting

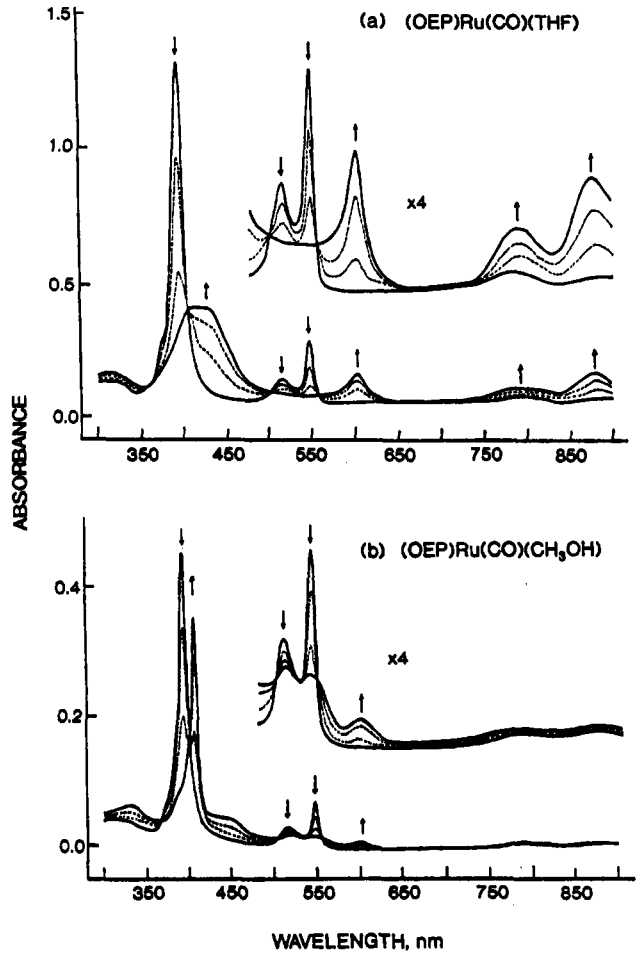

Figure 3. Time-resolved thin-layer UV–visible spectra obtained during controlled-potential reduction of (a) (OEP)Ru(CO)(THF) and (b) (OEP)Ru(CO)(CH_3OH) in THF containing 0.2 M TBAP at −1.9 V.

spectra under these solution conditions are shown in Figure 4.[20]

The reduction of (OEP)Ru(CO)(THF) was also monitored in THF that was not rigorously dried, and spectroelectrochemical results under these solution conditions are shown in Figure 5. The

(18) Kadish, K. M.; Lin, X. Q.; Ding, J. Q.; Wu, Y. T.; Araullo, C. *Inorg. Chem.* **1986**, *25*, 3236.

(19) The CH_3OH and H_2O content in THF was estimated to be 0.2 and 0.5%, respectively.

(20) A similar conversion between a Ru(I) type spectrum and that of a porphyrin π anion radical could also be obtained by addition of pyridine (10 equiv) or DMSO (200 equiv) to PhCN solutions containing (OEP)Ru(CO)(PhCN). The spectrum in neat PhCN was that of Ru(I), while the one obtained after reduction in PhCN containing pyridine or DMSO was that of a porphyrin π anion radical.

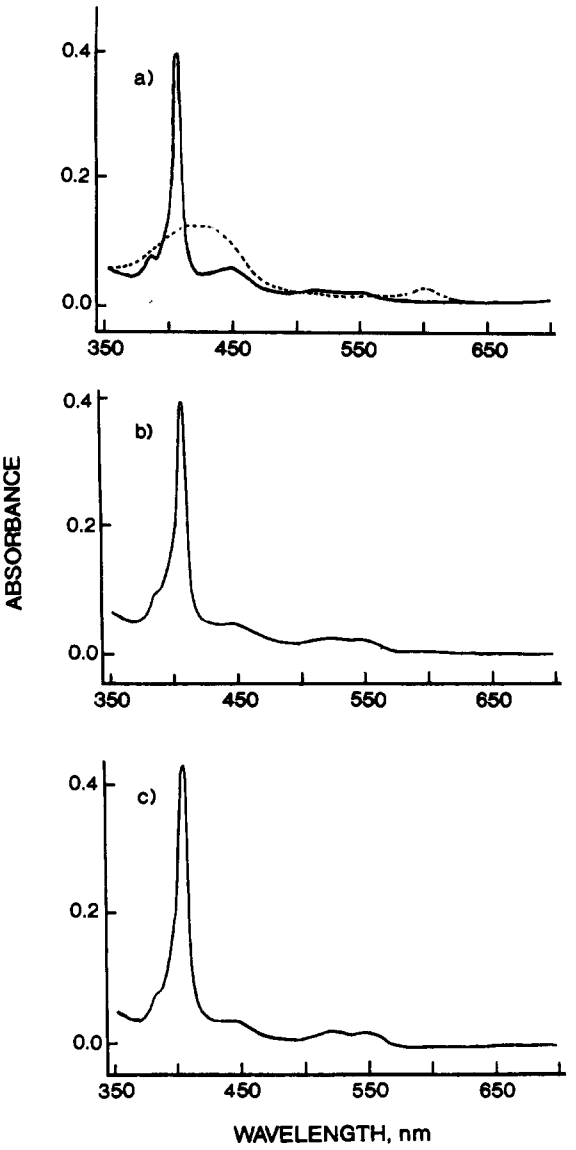

Figure 4. UV–visible spectra of (a) singly reduced (OEP)Ru(CO)(THF) (---) and (OEP)Ru(CO)(CH_3OH) (—) in THF, 0.2 M TBAP, (b) singly reduced (OEP)Ru(CO)(THF) in THF containing 0.2% CH_3OH, and (c) singly reduced (OEP)Ru(CO)(THF) in THF containing 0.5% H_2O.

addition of one electron is complete after about 2 min, and the spectrum at this time is characterized by a decreased intensity Soret band, a strong band at 601 nm, and additional broad bands between 786 and 880 nm. This spectrum continues to change with time after completion of the electrolysis, and this is illustrated by the insert in Figure 5, which plots absorbances for the 406- and 601-nm bands at times between 0 and 16 min after initiation of electrolysis. A radical type spectrum begins to form during the first 60 s after applying a controlled potential of −1.9 V, but after about 3 min the π-anion-radical character of the spectrum starts to disappear, as demonstrated by a decrease in intensity of the 601-nm band. The overall data are consistent with a slow conversion between two forms of the reduced metalloporphyrin, and this is also suggested by FTIR spectroelectrochemical data described in the following section.

FTIR Monitoring of (OEP)Ru(CO) Reduction in THF. Figure 6 illustrates the thin-layer FTIR spectra obtained before and after electroreduction of (OEP)Ru(CO)(THF) and (OEP)Ru(CO)-(CH_3OH) in THF. Both neutral ruthenium(II) porphyrins show a well-defined CO peak at 1931 cm^{-1}, and this agrees with data in the literature for other six-coordinate (OEP)Ru(CO)(L) complexes.[2] The spectrum of singly reduced (OEP)Ru(CO)-(THF) has a CO peak at 1878 cm^{-1}, while that of singly reduced (OEP)Ru(CO)(CH_3OH) shows a peak at 1896 cm^{-1}.

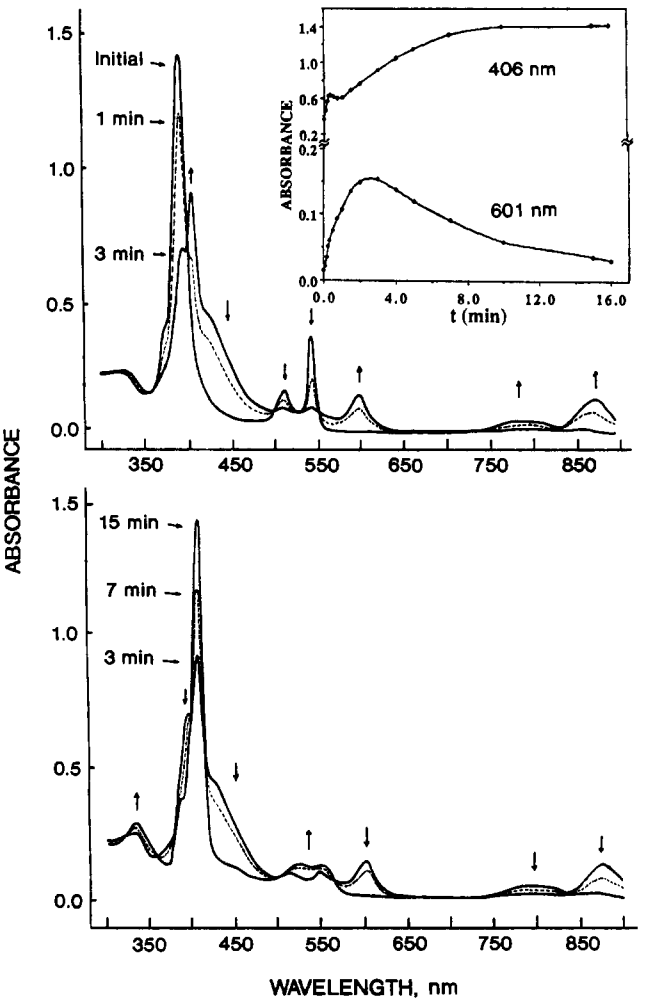

Figure 5. Time-resolved thin-layer UV–visible spectra obtained during controlled-potential reduction of (OEP)Ru(CO)(THF) at −1.9 V in wet THF containing 0.2 M TBAP.

The data in Figure 6 are consistent with two different reduced forms of the porphyrin, and this is further illustrated by time-resolved FTIR spectral data obtained during and after electroreduction of (OEP)(Ru)(CO)(THF) in wet THF (Figure 7). The initial IR spectrum obtained 0.5 min after applying a controlled potential of −1.9 V is characterized by a major peak at 1878 cm^{-1} and a shoulder at 1896 cm^{-1}. There is also a peak at 1931 cm^{-1} due to the unreduced starting material. This latter peak totally disappears after the reducing potential is applied for about 3 min, and at the same time, the 1878-cm^{-1} peak decreases as the 1896-cm^{-1} peak increases in intensity. The ratio of peak intensities continues to change at longer times (see spectrum after 10 min of electrolysis) and gives data consistent with a conversion between two reduced forms of the metalloporphyrin. As shown in Figure 7, the first observed electrogenerated species has a major CO peak at 1878 cm^{-1} and a shoulder at 1896 cm^{-1}, while the last measured spectrum has a major peak at 1896 cm^{-1} and a much smaller one at 1878 cm^{-1}.

UV–Visible and FTIR Monitoring of (OEP)Ru(CO) Oxidation. The electrooxidation of (OEP)Ru(CO)(L) was spectrally characterized in THF, CH_2Cl_2, and CH_2Cl_2 containing PhCN. The UV–visible changes obtained during controlled-potential oxidation of (OEP)Ru(CO)(THF) by one electron in THF are shown in Figure 8. The final electrogenerated product has a Soret band at 377 nm and one or more weak, broad absorption bands between 500 and 650 nm. This spectrum is characteristic of a metalloporphyrin π cation radical[21] and is similar to the UV–visible spectrum reported for electrogenerated $[(OEP)Ru(CO)]^+$ in

(21) Felton, R. H. In *The Porphyrins*; Dolphin, D., Ed.; Academic Press: New York, 1978; Vol. V, p 53.

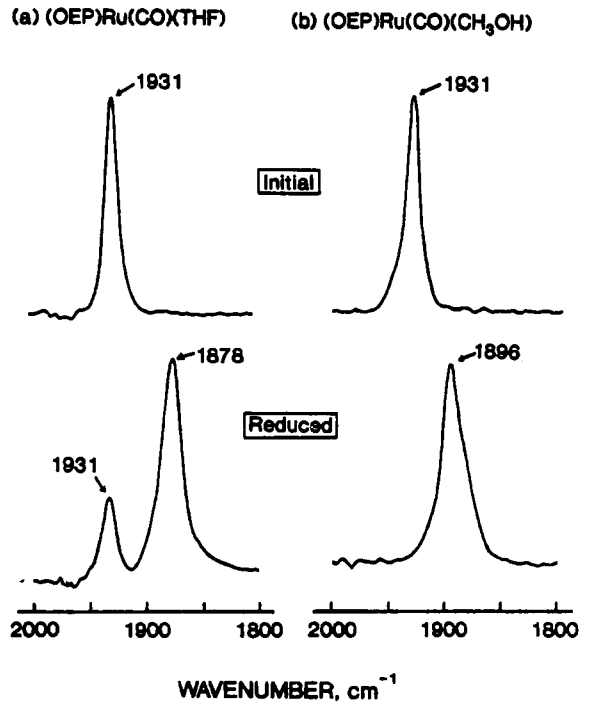

Figure 6. FTIR spectra of (OEP)Ru(CO)(THF) and (OEP)Ru(CO)-(CH_3OH) before and after controlled-potential reduction at −1.9 V in rigorously dried THF containing 0.2 M TBAP.

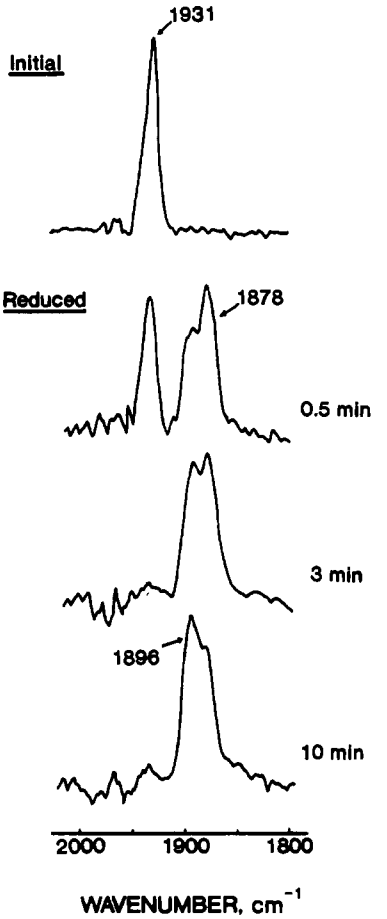

Figure 7. Time-resolved FTIR spectrum obtained during controlled-potential reduction of (OEP)Ru(CO)(THF) at −1.9 V in wet THF containing 0.2 M TBAP.

CH_2Cl_2.[8] Two well-defined isosbestic points are observed in Figure 8, and the process appears to correspond to a simple one-electron transfer as shown in eq 1.

$$(OEP)Ru(CO)(THF) \rightleftarrows [(OEP)Ru(CO)(THF)]^+ + e^- \quad (1)$$

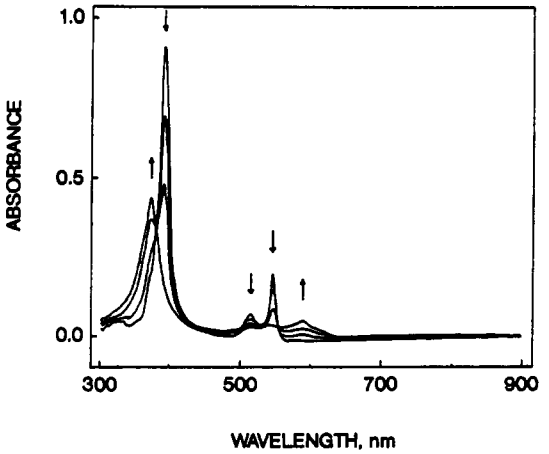

Figure 8. Time-resolved thin-layer UV–visible spectra obtained during controlled-potential oxidation of (OEP)Ru(CO)(THF) at 1.2 V in THF containing 0.2 M TBAP.

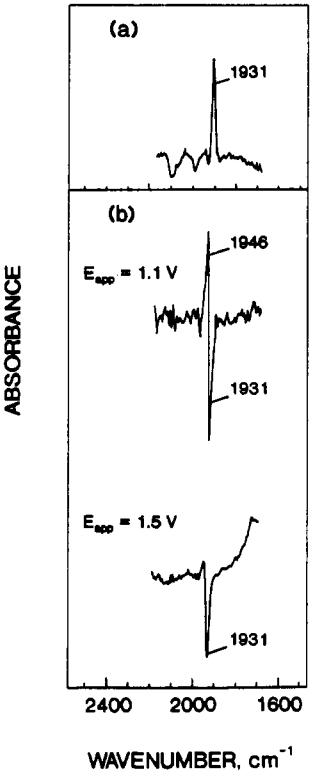

Figure 9. (a) Initial FTIR spectrum of (OEP)Ru(CO) in THF containing 0.2 M TBAP and (b) difference FTIR spectra after controlled-potential oxidation of (OEP)Ru(CO) at 1.1 and 1.5 V.

Isosbestic points are not observed if a further controlled-potential oxidation is carried out at 1.6 V, and the final UV–visible spectrum obtained at this potential is featureless. This indicates that $[(OEP)Ru(CO)(THF)]^{2+}$ is not the ultimate product of $[(OEP)Ru(CO)(THF)]^+$ oxidation and that a chemical reaction occurs after generation of the doubly oxidized species. It has already been reported that $[(OEP)Ru(CO)(L)]^{2+}$ undergoes decomposition,[6] and this reaction appears to occur on the spectroelectrochemistry time scale.

Figure 9 shows the thin-layer FTIR spectrum obtained before and after electrooxidation of (OEP)Ru(CO) in THF. The initial CO peak at 1931 cm^{-1} (Figure 9a) disappears as (OEP)Ru(CO)(THF) is converted to $[(OEP)Ru(CO)(THF)]^+$, which has a CO peak at 1946 cm^{-1} (see Figure 9b). A peak for complexed CO is not observed after electrooxidation at 1.5 V (the second oxidation), and this result is consistent with decomposition of the doubly oxidized product, as mentioned above.

The FTIR spectra obtained before and after oxidation of (OEP)Ru(CO) in neat CH_2Cl_2 and CH_2Cl_2 containing PhCN

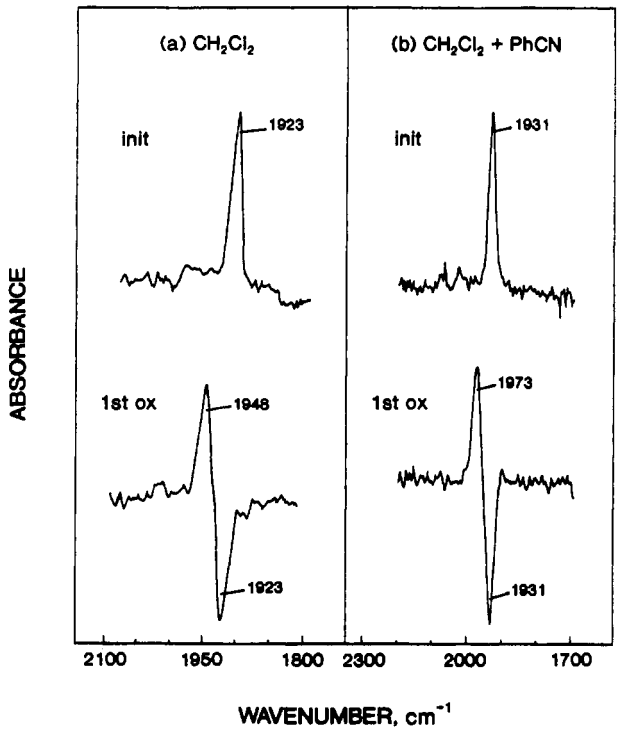

Figure 10. FTIR spectra obtained before and after oxidation of (OEP)Ru(CO) at 1.0 V in (a) CH_2Cl_2 containing 0.2 M TBAP and (b) CH_2Cl_2 containing 0.1 M PhCN and 0.2 M TBAP. The data after oxidation are presented as difference spectra.

Scheme I

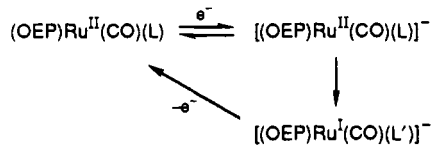

are shown in Figure 10. The initial CO peak is located at 1923 cm^{-1}, and this peak shifts to 1948 cm^{-1} after electrogeneration of $[(OEP)Ru(CO)]^+$. A CO peak is also observed at 1931 cm^{-1} for (OEP)Ru(CO) in CH_2Cl_2 containing 0.1 M PhCN (see Figure 10b), and this value is identical with the one measured for (OEP)Ru(CO)(PhCN) in neat PhCN. The neutral PhCN complex is converted to $[(OEP)Ru(CO)(PhCN)]^+$ upon oxidation at 1.0 V, and the spectral changes associated with this electrode reaction are shown in Figure 10b. A single CO peak is observed after electrooxidation, and this peak is located at 1973 cm^{-1}.

Discussion

Electroreduction of (OEP)Ru(CO)(L). Two different types of UV–visible spectra are obtained after electroreduction of (OEP)Ru(CO)(L). Both can be observed in THF (see Figures 3–5), and the resulting data in this solvent suggest an electron-transfer mechanism that occurs as schematically shown in Scheme I, where L and L′ are different axial ligands.

The initial electrogenerated product in Scheme I is a ruthenium(II) porphyrin π anion radical. This species is stable in pyridine, DMSO, or rigorously dried THF but is rapidly converted to a Ru(I) form of the complex in PrCN, PhCN, or CH_3CN. There is a slow conversion between the two reduced forms of the porphyrin in wet THF, and these time-dependent results are illustrated by the UV-visible and FTIR data in Figures 5 and 7. The porphyrin π anion radical bands in Figure 5 initially increase in intensity but after several minutes begin to decrease as a new well-defined Soret band starts to grow in at 406 nm. The data in this figure suggest the occurrence of an internal electron transfer from the reduced porphyrin π-ring system to the Ru(II) metal center of $[(OEP)Ru^{II}(CO)(L)]^-$, and the driving force for this internal electron transfer is postulated to be the exchange of an axial ligand (such as CH_3OH or H_2O for THF). The final electroreduced species is formulated as $[(OEP)Ru^{I}(CO)(L')]^-$ and can be converted to the initial unreduced $(OEP)Ru^{II}(CO)(L)$ complex by application of a positive controlled potential.

As mentioned above, the UV–visible spectra generated after reduction of (OEP)(Ru)(CO)(THF) in PrCN, PhCN, or CH_3CN are identical with spectra obtained after electroreduction in wet THF. They are also identical with the spectra produced in dry THF containing ~0.5% H_2O or ~0.2% CH_3OH (Figure 4) as well as with the spectrum formed after electroreduction of $(OEP)Ru(CO)(CH_3OH)$ in dry THF (Figure 3b). This suggests that the sixth axial ligand directly or indirectly determines the site of electron transfer.

No spectral evidence is observed for formation of a ruthenium(II) porphyrin π anion radical in the neat nitrile solvents, and this suggests a rapid chemical conversion between the two reduced forms of the porphyrin in PrCN, PhCN, or CH_3CN. There is also no spectral evidence that would indicate a direct conversion of $(OEP)Ru^{II}(CO)(L)$ to $[(OEP)Ru^{I}(CO)(L)]^-$, but this possibility cannot be totally ruled out on the basis of available data.

The FTIR spectroelectrochemical data in Figures 6 and 7 give further evidence for a mechanism of the type shown in Scheme I. The species generated after electroreduction of (OEP)Ru(CO)(THF) in dry THF (Figure 6) has a band at 1878 cm^{-1}, while electroreduction of $(OEP)Ru(CO)(CH_3OH)$ under the same solution conditions gives a spectrum with a well-defined peak at 1896 cm^{-1}. The 1878-cm^{-1} peak should correspond to CO of $[(OEP)Ru^{II}(CO)(L)]^-$, while the 1896-cm^{-1} peak would be associated with the coordinated CO of $[(OEP)Ru^{I}(CO)(L')]^-$. This assignment seems opposite to what is expected on the basis of metal oxidation state, but the related UV–visible data in Figure 5 clearly indicate that the first electrogenerated species is a porphyrin π anion radical, which is then converted to a final stable product containing an unreduced porphyrin π-ring system.

Attempts were made to measure CO peaks after electroreduction of (OEP)Ru(CO)(L) in each investigated solvent, but meaningful spectra could only be obtained in THF or pyridine, the latter of which shows a CO band at 1896 cm^{-1}. The lack of a well-defined spectrum in other solvents may have been due to a decomposition of the porphyrin or to a reduction of the solvent on the longer time scales needed for obtaining thin-layer FTIR spectra. In this regard, it should also be noted that the controlled potential needed for thin-layer electrolysis is close to the solvent potential limit and this could have led to the appearance of significant side reactions that give overlapping bands at longer time scales in the nitrile and DMSO solvents.

Electrooxidation of (OEP)Ru(CO)(L). The data on $[(OEP)Ru(CO)(L)]^+$ agree with what has been reported in the literature[5-8] and parallel results obtained for $[(TPP)Ru(CO)(L)]^+$ under similar experimental conditions. The singly oxidized OEP complexes all have CO peaks that are shifted by 15–42 cm^{-1} from the neutral species, and a similar trend has been noted for $[(TPP)Ru(CO)(L)]^+$ and (TPP)Ru(CO)(L), where shifts in ν_{CO} upon electrooxidation range between 23 and 43 cm^{-1}, depending upon the specific solvent.[11] The axially bound CO dissociates after the second oxidation of (OEP)Ru(CO)(L), and this also agrees with results reported in the literature.[11]

In summary, the UV–visible and FTIR spectroelectrochemical data indicate that the sixth axial ligand of (OEP)Ru(CO)(L) plays a significant role in determining the site of electron transfer during electroreduction in nonaqueous media. This has never before been demonstrated for reduction of a ruthenium(II) porphyrin. On the other hand, shifts in the site of metalloporphyrin electron transfer as a function of solvent or axial ligand are not novel and have earlier been reported for oxidation of several cobalt porphyrins in nonaqueous media.[22,23]

A comparison of data for singly reduced (OEP)Ru(CO)(L) with that of singly reduced(TPP)Ru(CO)(L)[11] also suggests that the site of electron transfer may vary as a function of the porphyrin

(22) Salehi, A.; Oertling, W. A.; Babcock, G. T.; Chang, C. K. *J. Am. Chem. Soc.* **1986**, *108*, 5630.
(23) Kadish, K. M. *Prog. Inorg. Chem.* **1986**, *34*, 437.

macrocycle basicity. Specifically, the eight electron-donating ethyl groups of (OEP)Ru(CO) should lead to an increased electron density on the porphyrin π-ring system, thus making electron addition to the central Ru metal relatively easier than electron addition to the porphyrin π-ring system. This is only a qualitative description. Other factors such as the donicity of the solvent may play some role in influencing the site of electron transfer. The Gutmann donor number increases from 11.9 to 16.6 upon going from PhCN to PrCN and from 20.0 to 33.1 upon going from THF to py.[24] An increase in donor number should result in more electron density on the central metal if the ligand is axially coordinated. Iterative extended Hückel calculations[1] show that the empty $d_{x^2-y^2}$ and d_{z^2} orbitals of the Ru ion in (OEP)Ru(CO)(py) have higher energy than that of the $e_g(\pi^*)$ orbital. Thus, the addition of one electron to the porphyrin π-ring system might be more favorable in this case.

Acknowledgment. The support of the National Science Foundation (Grant CHE-8822881) is gratefully acknowledged. We also acknowledge the help of Dr. John Bear with the thermogravimetric analysis experiments.

(24) Gutmann, V. *The Donor-Acceptor Approach to Molecular Interactions*; Plenum Press: New York, 1978.

Registry No. TBAP, 1923-70-2; THF, 109-99-9; DMSO, 67-68-5; py, 110-86-1; (OEP)Ru(CO)(PhCN), 135228-22-7; (OEP)Ru(CO)(CH_3CN), 135256-26-7; (OEP)Ru(CO)(PrCN), 135228-23-8; (OEP)Ru(CO)(THF), 55059-68-2; (OEP)Ru(CO)(DMSO), 112374-62-6; (OEP)Ru(CO)(py), 38478-17-0; [(OEP)Ru(CO)(PhCN)]$^-$, 135256-27-8; [(OEP)Ru(CO)(CH_3CN)]$^-$, 135228-24-9; [(OEP)Ru(CO)(PrCN)]$^-$, 135228-25-0; [(OEP)Ru(CO)(THF)]$^-$, 135228-26-1; [(OEP)Ru(CO)(DMSO)]$^-$, 135228-27-2; [(OEP)Ru(CO)(py)]$^-$, 135228-28-3; [(OEP)Ru(CO)]$^+$, 43145-33-1; [(OEP)Ru(CO)(PhCN)]$^+$, 135228-29-4; [(OEP)Ru(CO)(CH_3CN)]$^+$, 135228-30-7; [(OEP)Ru(CO)(PrCN)]$^+$, 135228-31-8; [(OEP)Ru(CO)(THF)]$^+$, 135228-32-9; [(OEP)Ru(CO)(DMSO)]$^+$, 135228-33-0; [(OEP)Ru(CO)(py)]$^+$, 80675-23-6; [(OEP)Ru(CO)(PhCN)]$^{2+}$, 135228-34-1; [(OEP)Ru(CO)(CH_3CN)]$^{2+}$, 135228-35-2; [(OEP)Ru(CO)(PrCN)]$^{2+}$, 135228-36-3; [(OEP)Ru(CO)(THF)]$^{2+}$, 135228-37-4; [(OEP)Ru(CO)(py)]$^{2+}$, 135228-38-5; [(OEP)Ru(CO)(py)]$^{2-}$, 135228-39-6; [(OEP)Ru(CO)]$^{2-}$, 135228-40-9; [(OEP)Ru(CO)(THF)]$^{2-}$, 135228-41-0; [(OEP)Ru(CO)(PrCN)]$^{2-}$, 135228-42-1; CH_2Cl_2, 75-09-2; PhCN, 100-47-0; CH_3CN, 75-05-8; PrCN, 109-74-0; (OEP)Ru(CO), 41636-35-5; (OEP)Ru(CO)(CH_3OH), 89530-39-2; [(OEP)Ru(CO)(CH_3OH)]$^-$, 135228-43-2.

Contribution from the Departamento de Química Inorgánica, Facultad de Ciencias, Universidad de Granada, 18071 Granada, Spain, Departamento de Química Inorgánica, Facultad de Ciencias, Universidad del País Vasco, Apartado 644, 48080 Bilbao, Spain, and UEI Cristalografía, Instituto Rocasolano, CSIC, 28006 Madrid, Spain

Gold(I) Phosphine Complexes: Mercaptooxopurine Base Interactions. Molecular and Crystal Structure of (8-Mercaptotheophyllinato-*S*)(triphenylphosphine)gold(I)

Enrique Colacio,*[†] Antonio Romerosa,[†] José Ruiz,[†] Pascual Román,*[‡] Juan M. Gutiérrez-Zorrilla,[‡] Angel Vegas,[§] and Martín Martínez-Ripoll[§]

Received December 13, 1990

The interaction of chloro(triphenylphosphine)gold(I) and [μ-1,2-bis(diphenylphosphino)ethane]bis[bromogold(I)] with mercaptooxopurine derivatives (8-mercaptotheophylline, 8-mercapto-2-thiotheophylline, and 8-(methylthio)theophylline) under basic conditions yields complexes of the type [Au(PPh_3)L], [{Au(PPh_3)}$_2$(μ-L)], [Au(μ-dppe)(μ-L)Au], and [LAu(μ-dppe)AuL] [L = mercaptooxopurine anion, dppe = 1,2-bis(diphenylphosphino)ethane], which contain either one S8-bonded or two N7,S8-bonded gold(I) phosphine groups. These complexes were characterized by means of ^{1}H, ^{13}C, and ^{31}P NMR and IR spectroscopy. Besides this, the crystal structure of the complex (8-mercaptotheophyllinato)(triphenylphosphine)gold(I) was determined from X-ray diffraction data. The compound crystallizes in triclinic space group $P\bar{1}$ with a = 8.035 (1) Å, b = 12.749 (5) Å, c = 13.172 (4) Å, α = 102.89 (5)°, β = 103.03 (2)°, γ = 103.77 (5)°, V = 1221.0 (8) Å^3, Z = 2, R = 0.037, and R_w = 0.039. The structure consists of neutral [Au(PPh_3)(HL^1)] (HL^1 = 8-mercaptotheophyllinato anion) held together in pairs by two N7-H---O6 hydrogen bonds and related by a crystallographic center of inversion. The coordination of the gold atom is almost linear, P-Au-S8 = 178.6 (2)°, with Au-S and Au-P bond distances of 2.308 (2) and 2.256 (2) Å, respectively. The substitution reaction between [Au(PPh_3)(HL^1)] and [($AuBr)_2$(μ-dppe)] to give the complex [Au(μ-dppe)(μ-L^1)Au] was studied. It seems that the reaction takes place through the intermediate complexes K[(L^1)Au(μ-dppe)AuBr]·4H_2O and [{Au(PPh_3)}$_2$(μ-L^1)].

Introduction

The current interest in the characterization of gold(I) phosphine complexes owes much to the successful use of the "auranofin", a gold(I) compound containing triethylphosphine and tetraacetylthioglucose ligands, for the treatment of rheumatoid arthritis.[1,2] In addition, auranofin and a number of Au(I) complexes of PPh_3 have been reported to have anticancer activity.[3-6] Likewise, 1,2-bis(diphenylphosphino)ethane (dppe) and some of its analogues have also been shown to have antitumor activity, and their activity is enhanced on coordination to gold(I).[7-11] In view of all this, the biological importance of purine bases and the possibility that gold binding to DNA bases could occur,[12,13] the study of (purine)gold(I) phosphine complexes is of interest. In a previous work[14] we have investigated the interaction of chloro(triphenylphosphine)gold(I) and [μ-1,2-bis(diphenylphosphino)ethane]bis[bromogold(I)] with a number of oxopurine bases and found the involvement of the deprotonated N-H groups in the complex formation, the N7 atom being the first binding

[†] Universidad de Granada.
[‡] Universidad del País Vasco.
[§] Instituto Rocasolano.

(1) Sutton, B. M.; McGusty, E.; Walz, D. T.; DiMartino, M. J. *J. Med. Chem.* **1972**, *15*, 1095.
(2) Weinstock, J.; Sutton, B. M.; Kuo, G. Y.; Walz, D. T.; Dimartino, M. J. *J. Med. Chem.* **1974**, *17*, 139.
(3) (a) Simon, T. M.; Kunishima, D. H.; Vibert, G. J.; Lorber, A. *Cancer* **1979**, *44*, 1965. (b) Simon, T. M.; Kunishima, D. H.; Vibert, G. J.; Lorber, A. *Cancer* Res. **1981**, *41*, 94.
(4) Mirabelli, C. K.; Johnson, R. K.; Sung, C. M.; Faucette, L.; Muirhead, K.; Crooke, S. T. *Cancer Res.* **1985**, *45*, 32.
(5) Sadler, P. J.; Nasr, M.; Narayanan, V. L. In *Platinum Coordination Complexes in Cancer Chemotherapy*; Hacker, M. P., Douple, E. B., Krakhoff, I. H., Eds.; Martinus Nijhoff Publishers: Boston, MA, 1984; pp 290-304.
(6) Shaw, C. F., III; Beery, A.; Stocco, G. C. *Inorg. Chim. Acta* **1986**, *123*, 213.
(7) Mirabelli, C. K.; Jensen, B. D.; Mattern, M. R.; Sung, C. M.; Mong, S. M.; Johnson, R. K.; Crooke, S. T. *Anticancer Drug Design* **1986**, *1*, 223.
(8) Mirabelli, C. K.; Hill, D. T.; Faucette, L. F.; McCabe, F. L.; Girard, G. R.; Bryan, D. B.; Sutton, B. M.; Bartus, J. O. L.; Crooke, S. T.; Johnson, R. K. *J. Med. Chem.* **1987**, *30*, 2181.

0020-1669/91/1330-3743$02.50/0